JOURNAL OF VIROLOGY, Sept. 2009, p. 8439–8450 Vol. 83, No. 17
0022-538X/09/$08.00+0 doi:10.1128/JVI.00877-09

Vaccinia Virus H7 Protein Contributes to the Formation of Crescent Membrane Precursors of Immature Virions[▽]

P. S. Satheshkumar, Andrea Weisberg, and Bernard Moss*

Laboratory of Viral Diseases, National Institute of Allergy and Infectious Diseases, National Institutes of Health, Bethesda, Maryland 20892-3210

Received 30 April 2009/Accepted 17 June 2009

Crescent membranes are the first viral structures that can be discerned during poxvirus morphogenesis. The crescents consist of a lipoprotein membrane and an outer lattice scaffold, which provides uniform curvature. Relatively little is known regarding the composition of the crescent membrane or its mode of formation. Here, we show that the H7 protein, which is conserved in all vertebrate poxviruses but has no discernible functional motifs or nonpoxvirus homologs, contributes to the formation of crescents and immature virions. Synthesis of the 17-kDa H7 protein was dependent on DNA replication and occurred late during vaccinia virus infection. Unlike many late proteins, however, H7 was not incorporated into mature virions or localized in cellular organelles. To gain insight into the role of H7, an inducible mutant was constructed and shown to have a conditional lethal phenotype: H7 expression and infectious virus formation were dependent on isopropyl-beta-D-thiogalactopyranoside. In the absence of inducer, viral late proteins were made, but membrane and core proteins were not processed by the I7 protease. A block in morphogenesis was demonstrated by transmission electron microscopy: neither typical crescents nor immature virions were detected in the absence of inducer. Instead, factory areas of the cytoplasm contained large, electron-dense inclusions, some of which had partially coated membrane segments at their surfaces. Separate, lower-density inclusions containing the D13 scaffold protein and endoplasmic reticulum membranes were also present. These features are most similar to those previously seen when expression of A11, another conserved nonvirion protein, is repressed.

The vertebrate poxviruses, of which vaccinia virus (VACV) is the prototype, encode about 200 proteins, of which almost half are conserved in all species (40). The conserved proteins include those that execute basic functions, which allow poxviruses to replicate and express their double-stranded DNA genomes and assemble infectious particles in the cytoplasm (25). Due to their large number, some of the conserved open reading frames (ORFs) have yet to be characterized. In the present study, we show that the product of the VACV H7R ORF contributes to the formation of the crescent membrane precursors of immature virions (IVs).

Crescents are uniformly curved membranes that form within specialized regions of the cytoplasm known as factories (8, 10). The crescents envelop electron-dense granular material containing core precursor proteins to form ~300-nm spherical IVs, which subsequently undergo internal and external architectural changes to become infectious brick-shaped mature virions (MVs) (6). Several models have been proposed for the structure and mode of formation of crescents and IVs. Transmission electron micrography revealed a single membrane bilayer covered with an external "spicule" coat (8, 24). Although evidence for two closely apposed membranes has been presented (29, 34), other studies support the original single membrane structure (5, 17–19). The outer coat was revealed by deep-etch immunogold electron microscopy to be a lattice comprised of trimers of the D13 protein (18, 36) rather than a layer of discontinuous spikes.

The crescent and IV membranes are not fully characterized with regard to their composition or organization, and two main theories regarding their origin have been proposed. One idea, inspired by the spatial separation of crescent and cellular membranes in virus factories, was the de novo origin of poxvirus membranes from lipids and viral proteins (9). An alternative model, positing the derivation of crescents from cellular membranes, was based partly on the lack of precedence of de novo membrane formation in other biological systems, the finding of some viral proteins associated with membranes of the intermediate compartment between the endoplasmic reticulum (ER) and the Golgi apparatus, and the proximity of tubular structures and viral membranes (29, 33). Other studies, however, provided evidence for trafficking of proteins to the viral membrane through the ER rather than the intermediate compartment although the initial membrane nucleation event was not investigated (20, 21).

Understanding the mechanism of viral membrane formation depends on the identification of the viral and cellular proteins involved. A role for the cellular coatomer and KDEL receptor in early VACV biogenesis has been suggested (43). Studies of conditional lethal VACV mutants pointed to the involvement of several viral proteins in the formation of crescent membranes. Repression of synthesis of the D13 scaffold protein mimics the effect of the drug rifampin and results in floppy-appearing membranes bordering electron-dense granular material (44). Such membranes seem otherwise normal as they can acquire the scaffold and concomitant rigid curvature within minutes after removal of rifampin and develop into IVs (26). Repression of synthesis of the integral membrane proteins A14

* Corresponding author. Mailing address: Laboratory of Viral Diseases, National Institute of Allergy and Infectious Diseases, National Institutes of Health, 33 North Drive, MSC 3210, Bethesda, MD 20892-3210. Phone: (301) 496-9869. Fax: (301) 480-1535. E-mail: bmoss@nih.gov.

▽ Published ahead of print on 24 June 2009.

and A17 results in aberrant vesicular or tubular structures that differ from each other in appearance (30, 31, 39, 41). Both A14 and A17 are phosphorylated by the F10 kinase (3, 13, 39), and viral membranes are not detected when cells are infected with conditional lethal F10 mutants under nonpermissive conditions (37, 38). Viral membranes are also not observed under nonpermissive conditions when cells are infected with conditional lethal H5 (12), G5 (7), and A11 (28) mutants though their roles in this process are not yet understood. Here, we characterize the product of the H7R ORF and demonstrate that it is also involved in viral membrane formation and morphogenesis.

MATERIALS AND METHODS

Cells and virus. BS-C-1 cells (ATCC CCL-26) were maintained in minimum essential medium with Earle's salts supplemented with 10% fetal bovine serum, 100 units of penicillin, and 100 μg of streptomycin per ml (Quality Biologicals, Gaithersburg, MD). The Western Reserve strain of VACV (ATTC VR1354) and the recombinant virus vT7LacOI (1) were propagated as described previously (14). MVs were purified by sedimentation twice through 36% sucrose cushions and banding once in a 25 to 40% sucrose density gradient (15).

Plasmid and recombinant VACV construction. Overlap PCR was used to assemble DNA segments for construction of plasmids and recombinant VACV. Transfections were carried out using Lipofectamine 2000 (Invitrogen, Carlsbad, CA). Recombinant viruses were clonally purified as described previously (16), and their structures were verified by PCR and DNA sequencing of relevant segments.

Plaque assay and virus yield determinations. For plaque assays, BS-C-1 cell monolayers in six-well tissue culture plates were infected with 10-fold serial dilutions of virus. After a 1-h adsorption, the medium containing unbound virus was removed and replaced with medium containing 0.5% methylcellulose with or without 150 μM isopropyl β-D-1-thiogalactopyranoside (IPTG). After 48 h, the infected cells were stained with crystal violet, and the plaques were counted.

For determinations of virus yield, BS-C-1 cells in 24-well dishes were incubated for 1 h with 3 to 5 PFU of virus per cell. After adsorption, the medium was removed, and the cells were washed and incubated in medium with or without 150 μM IPTG. Cells were harvested and lysed by multiple freeze-thaw cycles. Virus titers were determined by plaque assay in BS-C-1 cells in the presence of 150 μM IPTG.

Pulse-labeling of proteins with [^{35}S]methionine-cysteine. BS-C-1 cells were infected with 5 PFU of virus per cell and incubated at 37°C in medium with or without 150 μM IPTG. After 8 h, the medium was replaced with cysteine- and methionine-free medium for 30 min at 37°C and then pulse labeled for 15 min in medium containing 100 μCi of [^{35}S]methionine-cysteine (Perkin Elmer, Waltham, MA) per ml. Cells were harvested after the pulse-labeling period or washed and incubated with medium containing unlabeled methionine and cysteine for an additional 16-h chase and harvested. Whole-cell lysates were prepared in 1× NuPAGE lithium dodecyl sulfate sample loading buffer containing 1× reducing agent (Invitrogen) and heated at 100°C for 6 min. The proteins in the cell extracts were resolved in 4 to 12% Novex NuPAGE acrylamide gels (Invitrogen), dried, and analyzed by autoradiography.

Western blotting. Whole-cell lysates were prepared, and the proteins were resolved by gel electrophoresis on 4 to 12% Novex NuPAGE acrylamide gels as described above and transferred to nitrocellulose membranes using Mini iBlot gel transfer stacks (Invitrogen). The membrane was blocked with 5% nonfat milk in phosphate-buffered saline (PBS) containing 0.05% Tween-20 and then incubated with a primary antibody for 1 h at room temperature; the membrane was washed with PBS containing Tween-20 and then with PBS without detergent. For chemiluminescence detection, the appropriate secondary antibody conjugated with horseradish peroxidase (Pierce, Rockford, IL) was added, and the blot was washed and developed using Dura or Femto chemiluminescent substrate (Pierce). For fluorescent detection, donkey anti-mouse IRDye 800 and donkey anti-rabbit IRDye 680 were used and developed using a Li-Cor Odyssey infrared imager (Li-Cor Biosciences, Lincoln, NE). To reprobe the blots with different antibodies, the nitrocellulose membrane was stripped at 55°C for 20 min using Restore Buffer (Pierce). Goat antibody against the human influenza virus hemagglutinin (HA) epitope tag conjugated to horseradish peroxidase was obtained from Bethyl laboratories (Montgomery, TX). Anti-Flag M2 mouse monoclonal antibody (MAb) was from Sigma-Aldrich (St. Louis, MO). Rabbit polyclonal antibodies against A3 (R. Doms and B. Moss, unpublished data), A17 (41), and A28 (27) were used.

Confocal microscopy. HeLa cells grown on coverslips were infected for 18 h, fixed with 4% paraformaldehyde, and permeabilized with PBS containing 0.1% Triton X-100. The sample was blocked with 10% fetal bovine serum, followed by incubation with primary antibodies in serum for 1 h. Cells were washed with PBS and incubated with appropriate secondary antibodies conjugated to dyes (Molecular Probe, Eugene, OR) for an additional 1 h. Coverslips were washed and mounted on a glass slide using Prolong Gold (Invitrogen).

Electron microscopy. For conventional transmission electron microscopy, infected BS-C-1 cells in 60-mm-diameter wells were fixed with 2% glutaraldehyde and embedded in EmBed-182 resin (Electron Microscopy Sciences, Hatfield, PA). Procedures for cryosectioning and immunogold labeling were described previously (32). Specimens were viewed with FEI-CM100 and FEI Tecnai Spirit transmission electron microscopes (FEI, Hillboro, OR).

RESULTS

H7 synthesis is dependent on DNA replication and occurs at late times. All chordopoxviruses that have been sequenced encode a homolog of the VACV H7R ORF that varies from 138 to 152 amino acids in length. Multiple alignments indicate that 96 to 100% of the H7 amino acid sequence is conserved among orthopoxviruses and that 37 to 44% is conserved among other chordopoxvirus genera (Fig. 1). The calculated pI of H7 is 6.74, and there is no putative transmembrane domain, signal peptide, coiled-coil segment, or structural features that could be discerned from the amino acid sequence. Immediately preceding and overlapping the start of the H7R ORF is the nucleotide sequence TAAATG, indicative of a late promoter.

In order to study expression and protein interactions in the absence of specific antibodies, a recombinant VACV with affinity and epitope tags attached to H7 was generated by homologous recombination. The H7R ORF was modified to encode three copies of a Flag (3×Flag) tag and streptavidin-binding peptide in tandem at the N terminus, without altering the H7R promoter sequence or its location within the genome. The green fluorescent protein (GFP) ORF regulated by the VACV F17R late promoter was inserted to the left of the H7R ORF and in the opposite orientation to assist in the isolation of the recombinant virus. These modifications are shown in Fig. 2A. Following infection with the VACV Western Reserve strain and transfection with the PCR product, recombinant virus plaques were identified by fluorescence microscopy and clonally purified. The plaques of the recombinant virus v3×Flag-SBP-H7 (abbreviated as vFS-H7) were similar in size to those of the parental virus (data not shown), indicating that this genetic manipulation did not adversely affect replication.

Synthesis of H7 was determined by infecting BS-C-1 cells with vFS-H7 for various times and analyzing the proteins in lysates by polyacrylamide gel electrophoresis (PAGE). Western blotting was performed using anti-Flag M2 mouse MAb to detect H7 and rabbit polyclonal antibody to the well-characterized A3 late protein, followed by anti-mouse and anti-rabbit fluorescent secondary antibodies so that the proteins could be analyzed on the same gel. The expected-size precursor and product A3 polypeptides were detected at 9 h and increased with time (Fig. 2B). The 17-kDa H7 protein exhibited a similar late time course of synthesis and accumulation (Fig. 2B). Neither A3 nor H7 was detected even at 24 h when DNA replication was blocked with cytosine arabinoside (AraC) (Fig. 2B). Thus, the promoter sequence, kinetics of synthesis, and re-

```
GTPV   --MDERLKTISMTFFYGELTTTDIMVLKAHLLNIFPNDTIFSINE-DNKFIIDFKYND-C 56
SWPV   --MDERLRTISMTFFSGELNTIDIMMLKSYLLGIEPSDTIFSINKKNNNFVMNFKYDS-C 57
MYXV   --MDERFKTLALTFFSGELTTTDVMALKLHLLDTAPTDTVFCTDE-NNKFMIDYKYET-C 56
YMTV   --MDDKLKTISLTFFSGELSPVDIVAIKLFLLNKRPIETVFSIDG-KNNFVLDFNYGS-F 56
FWPV   --MDHKSRMLLDTIFKDMLNTKDVYALIKYIFKKDPVETIFSKKD--DDIFIDFVYNDNV 56
VACV   MEMDKRMKSLAMTAFFGELSTLDIMALIMSIFKRHPNNTIFSVDK-DGQFMIDFEYDN-Y 58
VARV   MEMDKRMKSLAMTAFFGELTTLDIMALIMSIFKRHPNNTIFSVDK-DGQFMIDFEYDT-Y 58
MOCV   --MDADLKLLAETLFAGVLSTKDVYVLAREMRGQSPRRTVFSVDA-QGCVGVDFEYDG-F 56
ORV    --MDEALRVAARVVDG--LRPLDVAVCLVQLRGAAPERRFPALDERSGEAFLDFEFAGGD 56
         **   :    .     * . *:      :    *   . . .   .   ::: :

GTPV   LASGYINQKIIPITPEKYNEYSSMIAKELTNYNIIIDDIKGHILSSKKLKRFIKFY-KTN 115
SWPV   LASDYINEIIEPIVPEDYPVYSPMIAKELTNYDIICDDIDTYISSSKKLKRVIKFY-KTN 116
MYXV   LTSHYLNKKTKSIQPDQYQKYSPAIATELTNYDIILEDVCAYINESRVLKRFVKLY-KTN 115
YMTV   LASNYTNINLKRLQRDEYIVYSSDIAKELTLYDIICDNVQDYINNSSKLKRVVKIY-KCK 115
FWPV   LASDYLGMKTTKV--EDCCSCRKVVAVEYMNTSIIDNDLEGYIKQSDKLKRFIKLYNKNN 114
VACV   KASQYLDLTLTPISGDECKTHASSIAEQLACVDIIKEDISEYIKTTPRLKRFIKKY---- 114
VARV   KASQYLDLPLTPISGDECKTHASSIAKQLACVDIIKEDISEYIKTTPRLKRFIKKY---- 114
MOCV   RASDYLGTPRTALPPAEYRAHAALVARELTAVDMIDEDPAAYMRASPHLRRLMRVA---- 112
ORV    VASRYLSAHTRELCAAERREHMAAIARCVTEADLALAD-----RPRGKARAALRVC---- 107
        :* * .     :   .       :*      .:   :           :  ::

GTPV   NNKQNKKIINASKKLNIALNKGIDYDYIRHIN------ 147
SWPV   SDKHNKRINEANKKLKIALSKGIDYDYIKGTCT----- 149
MYXV   NRKQNIKIIEASKRLKIALNKGIDYDYIKEVF------ 147
YMTV   --KQNIKIKEARKSLKIATKRGVDYDYIKDSCVLNSR- 150
FWPV   AIKKARNIKSRQKMLKDAGIDDIGYEFIKDAIGLISRK 152
VACV   RNRSDTRISRDTEKLKIALAKGIDYEYIKDAC------ 146
VARV   RNRSDTRISQDTEKLKIALAKGIDYEYIKDAC------ 146
MOCV   --RDRKRMAAIARTQQRAARRGLDCAFIKDVVF----- 143
ORV    --RNREKVSRLARLLRDAESSGADFAFIRAAVV----- 138
         :   .:    .  . *   . .  :*:
```

FIG. 1. Multiple sequence alignment of H7 orthologs of chordopoxviruses. Representative sequences from each genus of the family *Chordopoxvirinae* are included in the alignment. GTPV, goatpox virus strain Pellor; SWPV, swinepox virus strain Nebraska; MYXV, myxoma virus strain Lausanne; YMTV, yaba monkey tumor virus stain Amano; FWPV, fowlpox virus stain Iowa; VARV, variola virus strain Bangladesh; MOCV, molluscum contagiosm virus strain subtype 1; ORV, Orf virus strain OV-SA00. Completely and highly conserved amino acids are depicted by stars and colons, respectively.

quirement for DNA replication were consistent with the classification of H7 as a late protein.

H7 was not incorporated into virions or retained in viral factories. To determine whether H7 was packaged in virions, HeLa cells were infected with vFS-H7. MVs were purified from cytoplasmic extracts by sedimentation through two successive sucrose cushions followed by sucrose density gradient centrifugation. H7 was detected in the cell extract by sodium dodecyl sulfate (SDS)-PAGE and Western blotting but not in the pellet from the sucrose cushion or in purified virions (Fig. 2C). As a control, the blot was stripped and reprobed with antibody against A3, a virion core protein. This protein was detected predominantly as the precursor in the cell extract, and the cleaved product was detected in the cushioned and sucrose gradient purified virions (Fig. 2C). Based on the staining intensities of proteins in extracts and purified virions, we concluded that little or no H7 was packaged relative to A3, even though the two proteins exhibited the same kinetics of synthesis.

The intracellular location of H7 was determined by confocal microscopy following infection with vFS-H7. Cytoplasmic factories were located by staining DNA with 4′,6-diamidino-2-phenylindole (DAPI). H7 and the membrane protein L1 were detected with M2 MAb and polyclonal rabbit antibody, respectively, followed by secondary fluorescent antibodies. In addition, GFP expressed by a late promoter in vFS-H7 and a control replication-competent virus vI5-HA (35) was imaged. At 6 and 9 h after infection, GFP was detected in viral factories, which are the sites of late protein synthesis, as well as elsewhere in the cell (Fig. 3). At these times, L1 was predominantly in the factory (Fig. 3). H7 was detected in the factory but also throughout the cell (Fig. 3). The latter was not due to background, as shown by the faint staining of the control cells infected with vI5-HA (Fig. 3). At 12 and 24 h, GFP and H7 were more dispersed than L1, which was mainly in factories and punctate structures probably representing virions (Fig. 3). Taken together, the biochemical and microscopy data suggested that H7 was synthesized in virus factories but did not localize in virions or specific cellular organelles.

H7 is essential for virus replication. The conservation of H7 homologs in all chordopoxviruses suggested an essential role in virus replication. This prediction was supported by our inability to replace the H7 gene with GFP by homologous recombination. We therefore constructed a recombinant VACV in which the native H7R gene was replaced with one that is regulated by a bacteriophage T7 promoter and *Escherichia coli lac* operator (Fig. 4A). The parent virus, vT7LacOI, contains both the *E. coli lac* repressor and the phage T7 RNA polymerase in the

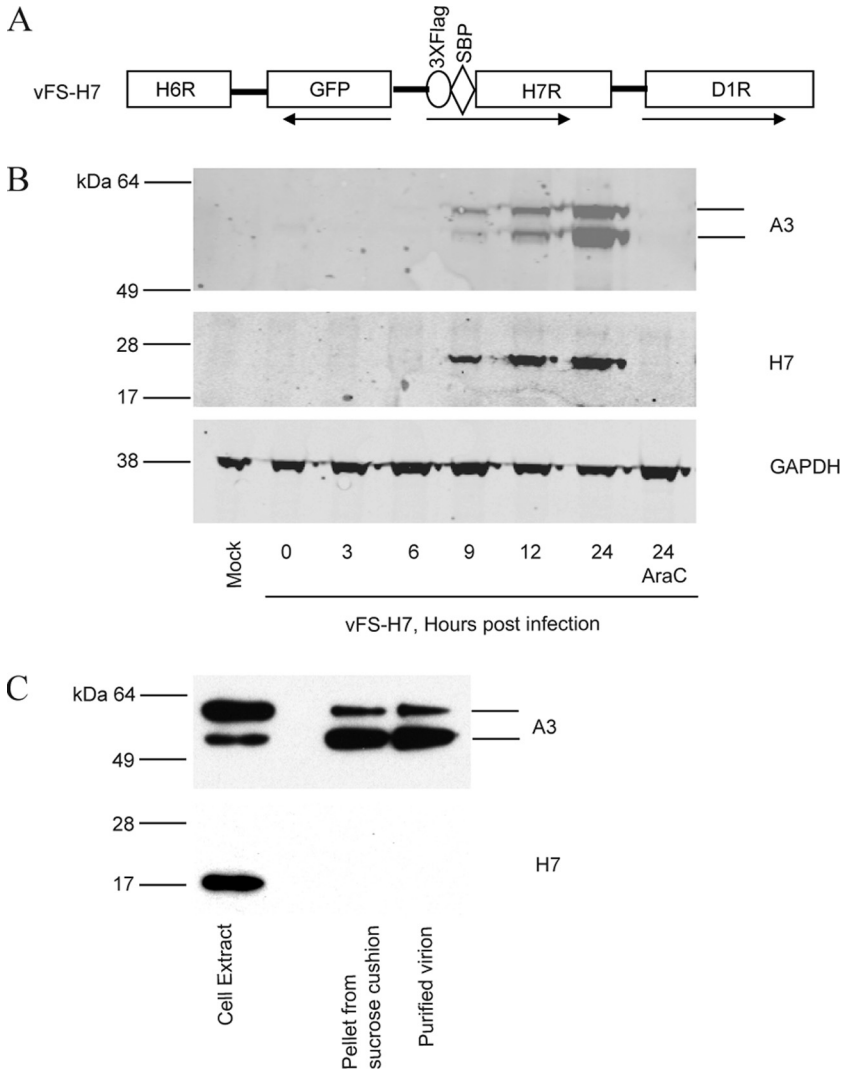

FIG. 2. Expression of H7. (A) Schematic representation of a portion of the genome of recombinant VACV vFS-H7. ORFs are indicated by boxes, and the directions of transcription are indicated by arrows. The 3×Flag and streptavidin-binding peptide (SBP) tags are fused to the N terminus of H7. (B) Expression of H7. BS-C-1 cells were mock infected or infected with vFS-H7 in the absence or presence of AraC and harvested at indicated times after infection. Whole-cell lysates were analyzed by SDS-PAGE, and the proteins were transferred to a membrane and probed with anti-Flag M2 mouse MAb to detect H7 and a rabbit polyclonal antibody to A3, followed by mouse- and rabbit-specific fluorescent secondary antibodies. Fluorescent images are shown. The blot was then stripped and reprobed with antibody to glyceraldehyde-3-phosphate dehydrogenase (GAPDH) as a loading control. (C) Analysis of purified MVs. Cells infected with vFS-H7 were lysed, and MVs were purified by sedimentation twice through sucrose cushions and a sucrose gradient. Fractions of the cell lysate, pellet from the second sucrose cushion, and purified virions were analyzed by SDS-PAGE and Western blotting using antibodies to the Flag epitope to detect H7 and specific antibody to A3. The bands were detected by chemiluminescence.

J2R (thymidine kinase) locus (1). The repressor is expressed constitutively by tandem early and late promoters, whereas the polymerase is inducible because of a *lac* operator that regulates a late promoter. The recombinant virus was constructed in two steps. First, an H7 gene with a C-terminal influenza virus HA epitope tag was inserted adjacent to the T7 promoter and *lac* operator in the pVote 1 plasmid transfer vector, which contains A56R flanking sequences for recombination into the VACV HA gene and *E. coli* guanine xanthine phosphoribosyl transferase to enable antibiotic selection (1). The plasmid was transfected into cells that were infected with vT7lacOI, and the intermediate recombinant virus vH7R/H7-HAi was selected with mycophenolic acid. In the next step, the endogenous H7R gene was replaced with GFP by homologous recombination in the presence of IPTG and the fluorescent virus, vH7-HAi, containing a single H7 gene with an inducible promoter was clonally purified.

vH7-HAi produced plaques only when IPTG was present in the medium, indicating that expression of H7 was essential for the replication or virus spread (Fig. 4B). The stringency was confirmed by the finding of only single infected cells by fluorescence microscopy in the absence of inducer (Fig. 4B). The effect of IPTG concentration on infectious virus formation was measured in order to distinguish whether H7 was required for VACV replication or spread. Replication of vH7-HAi depended on IPTG, with the optimal virus yield at 100 μM or

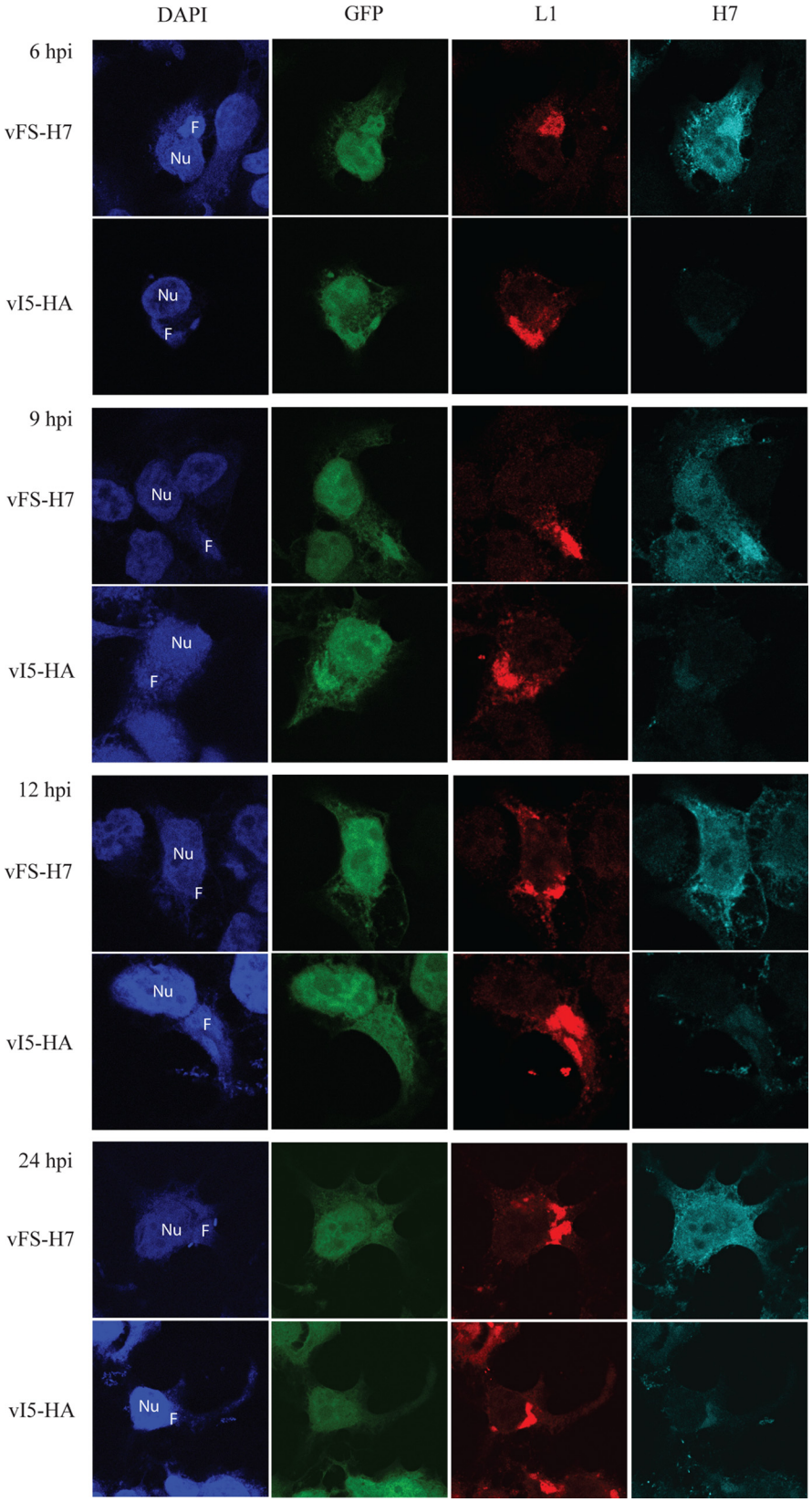

FIG. 3. Localization of H7 in infected cells by confocal microscopy. HeLa cells grown on coverslips were infected with either vFS-H7 or control vI5-HA virus (35). The vI5-HA virus was chosen as a control because it shows no defect in replication and expresses GFP. At 6, 9, 12, and 24 h, the cells were fixed and permeabilized. L1 and H7 were detected with a mouse MAb and rabbit polyclonal antibody, respectively, followed by species-specific fluorescent secondary antibodies. DNA was stained with DAPI. Nu, nucleus; F, viral factory; hpi, hours postinfection.

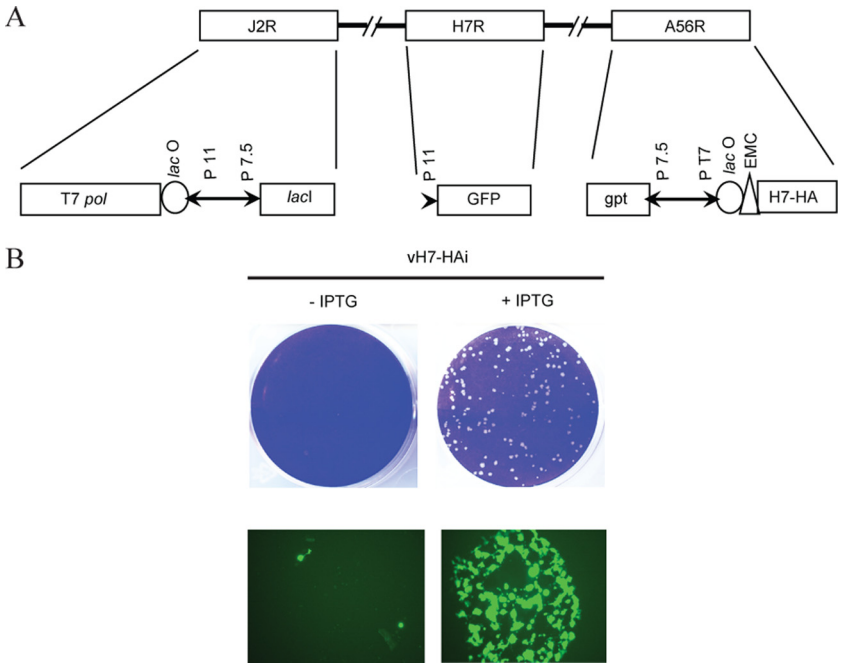

FIG. 4. Construction and initial characterization of a conditional lethal H7 mutant. (A) Diagram of a portion of the genome of vH7-HAi. T7*pol*, bacteriophage T7 RNA polymerase; *lac*O, *lac* operator; P11, a VACV late promoter; P7.5, a VACV early/late promoter; *lac*I, *E. coli lac* repressor gene; GFP, enhanced GFP gene; *gpt*, *E. coli* guanine phosphoribosyltransferase gene; PT7, bacteriophage T7 promoter; EMC, encephalomyocarditis virus cap-independent translation enhancer element. (B) Plaque morphology of vH7-HAi. BS-C-1 cells were infected with vH7-HAi in the presence or absence of 150 μM IPTG. Plaques were visualized after 48 h by staining with crystal violet. Color images of unstained plates examined after 24 h with a fluorescence microscope are also shown. The image on the left shows fluorescence of individual cells in the absence (−) of IPTG, and the image on the right is of a single plaque formed in the presence (+) of IPTG.

higher, whereas vT7LacOI was insensitive to IPTG (Fig. 5A). Replication of vH7-HAi correlated with synthesis of H7-HA as determined by Western blotting (Fig. 5A). One-step growth experiments confirmed the stringent requirement of IPTG for replication of vH7-HAi, with only a slight increase in titer at 24 h (Fig. 5B).

Complementation experiments were carried out to prove that the defect in vH7-HAi replication in the absence of IPTG was specifically due to repression of H7. Cells were infected with vH7-HAi in the absence of IPTG and then transfected with a plasmid containing the H7R gene under its natural promoter. Nearly a 10-fold increase in infectious virus was achieved over that in untransfected cells or in control HcRed plasmid-transfected cells (Fig. 5C).

H7 expression is essential for proteolytic processing of membrane and core proteins. To analyze the effect of H7 on VACV protein synthesis and processing, infected cells were labeled with radioactive amino acids using a pulse-chase protocol. BS-C-1 cells were infected with the parental virus vT7LacOI in the absence and presence of rifampin and with vH7-HAi in the absence and presence of 100 μM IPTG. Rifampin is an inhibitor of VACV morphogenesis that prevents proteolytic maturation of core proteins. After infected cells were labeled for 15 min with [^{35}S]methionine-cysteine, whole-cell extracts were analyzed by SDS-PAGE followed by autoradiography. Repression of H7 did not affect viral late protein synthesis (Fig. 6A). After the chase, the band pattern in the absence of H7 was similar to that of vT7LacOI infection in the presence of rifampin, suggesting that proteolytic processing was inhibited (Fig. 6A).

To confirm the pulse-chase result, proteolytic processing was monitored by Western blotting with specific antibodies. BS-C-1 cells were infected with vT7LacOI or vH7-HAi in the absence and presence of 100 μM IPTG. As expected, H7 was detected in only the extracts of cells infected with vH7-HAi in the presence of IPTG (Fig. 6B). Antibodies to the membrane protein A17 bound to two bands in extracts from cells infected with vT7LacOI and vH7-HAi in the presence of 100 μM IPTG due to proteolytic processing of the protein by the I7 protease (2). In the absence of IPTG, only the upper band corresponding to uncleaved A17 was detected (Fig. 6B). Similarly, the core protein A3 was resolved as two bands representing precursor and processed forms in cells infected with vT7LacOi and vH7-HAi in the presence of 100 μM IPTG. However, when H7 was repressed in the absence of IPTG, only the upper unprocessed band was detected (Fig. 6B). These results demonstrated that proteolytic maturation of membrane and core protein steps was inhibited in the absence of H7, suggesting an early block in morphogenesis.

During VACV infection, MV membrane proteins are not glycosylated even though they may have potential glycosylation sites. However, some of these membrane proteins are glycosylated when viral membrane formation is inhibited, presumably due to aberrant intracellular trafficking (23, 28). The mobility of A28, one of the MV membrane proteins, was slower than normal when H7 was repressed in cells infected with vH7-HAi in the absence of

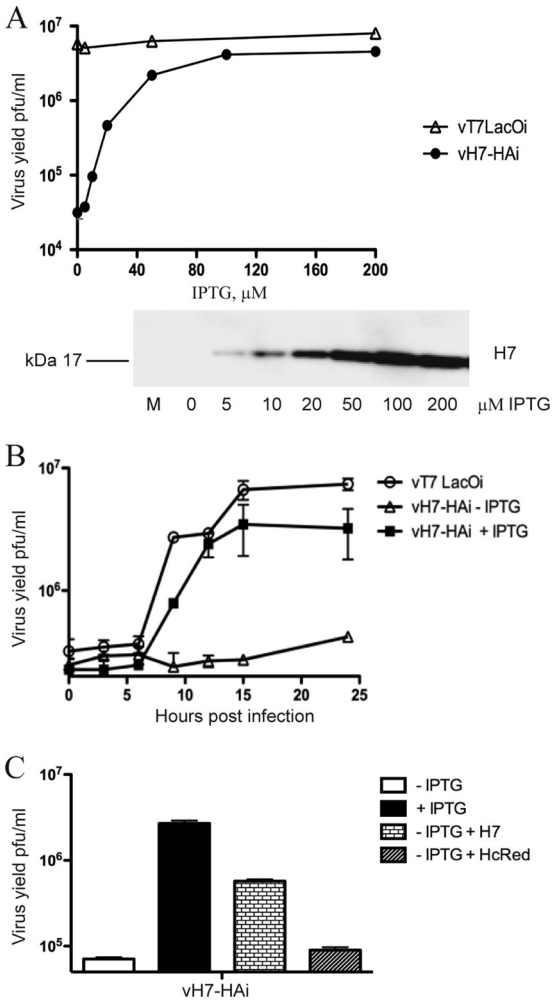

FIG. 5. Dependence of vH7-HAi replication on IPTG. (A) IPTG concentration. BS-C-1 cells were infected with vH7-HAi or vT7LacOI at 3 PFU per cell in the presence of 0 to 200 μM IPTG. Cells were harvested after 24 h and lysed, and virus titers were determined by plaque assay in BS-C-1 cells in the presence of 150 μM IPTG. In a parallel experiment, lysates were analyzed by Western blotting with antibody to the HA epitope tag. The bound protein was detected by chemiluminescence. (B) One-step growth kinetics. BS-C-1 cells were infected with 3 PFU per cell of vT7LacOI or vH7-HAi in the absence (−) or presence (+) of 150 μM IPTG. Cells were harvested at indicated times and lysed by freezing and thawing, and the virus titers were determined by plaque assay in the presence of 150 μM IPTG. (C) Complementation of vH7-HAi replication. BS-C-1 cells were infected with vH7-HAi virus at 3 PFU per cell in the absence or presence of 150 μM IPTG. After 1 h, cells infected in the absence of IPTG were transfected with a plasmid expressing either H7-HA under its natural promoter or control plasmid expressing HcRed under the P7.5 promoter. Cells were harvested at 24 h after infection, and the viral titer was determined by plaque assay in BS-C-1 cells in the presence of 150 μM IPTG.

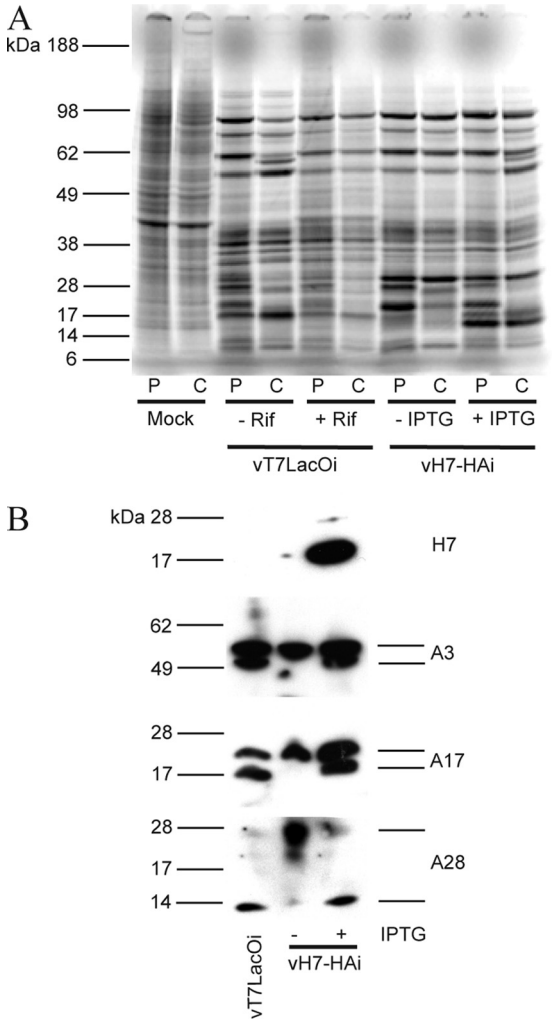

FIG. 6. Synthesis and processing of membrane and core proteins. (A) Pulse-chase analysis. BS-C-1 cells were infected with 3 PFU per cell of vT7LacOI in the absence (−) or presence (+) of 100 μg/ml of rifampin or vH7-HAi in the absence (−) or presence (+) of 150 μM IPTG. After 8 h, infected and mock-infected cells were pulse labeled for 15 min with [^{35}S]methionine-cysteine and either harvested immediately or after a 16-h chase in unlabeled medium. The whole-cell lysates were analyzed by SDS-PAGE, and the gel was dried and exposed to X-ray film for autoradiography. P, pulse; C, chase; Rif, rifampin. The positions and masses of protein standards are on the left. (B) Proteolytic processing of core and membrane proteins. BS-C-1 cells were infected with 3 PFU per cell of vT7LacOI or vH7-HAi in the absence or presence of 150 μM IPTG. Cells were harvested after 24 h, lysed in sample loading buffer, resolved on polyacrylamide gels, and transferred to a nitrocellulose membrane. Probing of the Western blot was performed first with antibody against the HA epitope on H7. The membrane was stripped and reprobed with antibodies against the A3, A17, and A28 proteins.

inducer (Fig. 6B). Peptide:*N*-glycosidase F treatment confirmed that the slow mobility was due to glycosylation (data not shown).

Cytoplasmic inclusions containing core proteins formed when H7 was repressed. When examining confocal fluorescence microscopy images of cells infected with vH7-HAi in the absence of IPTG, we noted peculiar dense GFP inclusions as large as 1.5 to 2.5 μm in diameter within the DAPI-staining virus DNA factories (Fig. 7A). These inclusions were poorly stained with antibody to GFP, apparently due to failure of the primary or secondary antibodies to penetrate into the interior of the mass (Fig. 7A). In the presence of IPTG, GFP was more diffusely localized in the cytoplasm and nucleus, as shown by both intrinsic fluorescence and antibody staining (Fig. 7A). To further investigate this observation, vH7-HAi-infected cells were stained with antibodies to the MV membrane protein L1 and the core protein A4. In the absence of IPTG, both proteins

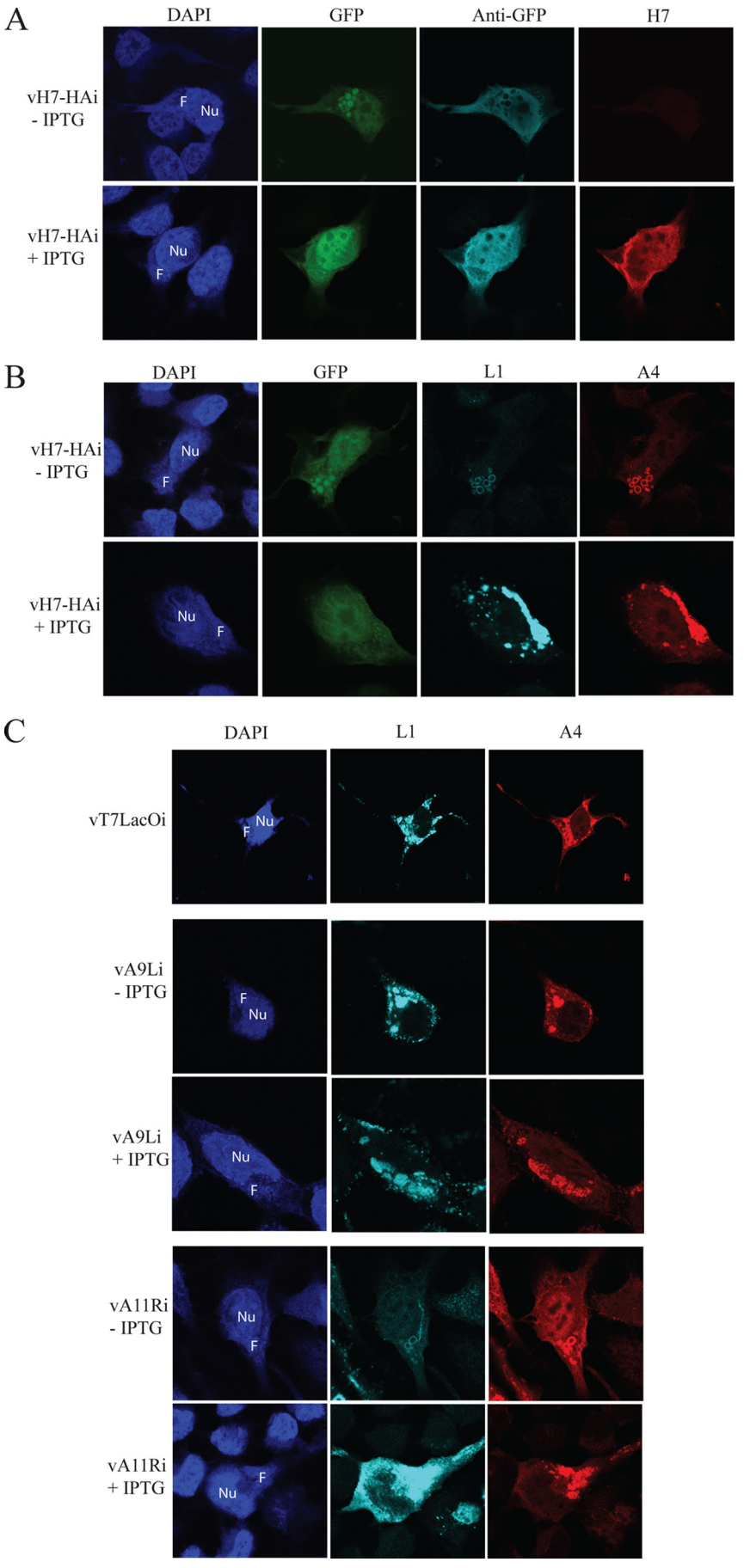
A
DAPI
GFP
Anti-GFP
H7
vH7-HAi
- IPTG
vH7-HAi
+ IPTG
Nu
F
B
DAPI
GFP
L1
A4
vH7-HAi
- IPTG
vH7-HAi
+ IPTG
Nu
F
C
DAPI
L1
A4
vT7LacOi
vA9Li
- IPTG
vA9Li
+ IPTG
vA11Ri
- IPTG
vA11Ri
+ IPTG
Nu
F

colocalized with the GFP inclusions in factories but appeared as ring structures due to the inability of the stain to penetrate (Fig. 7B). However, in the presence of IPTG, these proteins stained the factories diffusely, with some punctate staining of virus particles in the cytoplasm (Fig. 7B) similar to that of the parental vT7LacOI (Fig. 7C). The staining of L1 was much weaker in cells infected with vH7-HAi in the absence of IPTG than in the presence of IPTG, and this correlated with low levels of the protein on Western blots (data not shown).

We compared the results obtained with the conditional lethal H7 virus with two other mutant viruses that have blocks in morphogenesis. Repression of A9 interferes with the morphogenesis of IVs (42), whereas repression of A11 prevents IV formation (28). In the absence and presence of IPTG, L1 and A4 colocalized in cells infected with the inducible A9 mutant, but ring structures were not seen (Fig. 7C). However, the pattern obtained with the A11 mutant was similar or identical to that obtained with the H7 mutant, i.e., rings that stained with L1 and A4 antibodies in virus factories (Fig. 7C). L1 stained only weakly in cells infected with the A11 mutant in the absence of IPTG, as seen above with the H7 mutant.

Crescent membrane and IV formation are dependent on H7 expression. To better understand the replication block, morphogenesis of VACV in cells infected with vH7-HAi was investigated by transmission electron microscopy. The entire spectrum of normal morphological forms of VACV including crescents, IVs, MVs, and wrapped virions was observed in thin sections of cells infected with vH7-HAi in the presence of IPTG (Fig. 8A). In contrast, up to 1.5-μm-diameter inclusions were seen in thin sections of cells infected with vH7-HAi in the absence of IPTG (Fig. 8B). The prominent inclusions contained electron-dense granular material resembling the viroplasm of IVs. Small membrane arcs partially coated with spicules, which resembled the longer crescents, were seen at the surface of some dense inclusions (Fig. 8C and D).

Identification of protein components of cytoplasmic inclusions. Cryosections were stained with antibodies followed by protein A-gold in order to further characterize the inclusions. The electron-dense inclusions stained with antibody to the A3 (p4b) core protein, indicating that it corresponds to the granular material normally found within IVs (Fig. 9C). Based on size and presence of core proteins, the electron-dense inclusions appear to correspond to the ring structures seen by confocal microscopy. Intermediate electron density inclusions that stained with antibody to D13, the IV scaffold protein, were also seen (Fig. 9A). Membranes within and around the intermediate-density inclusions stained with antibody to protein disulfide isomerase, an ER-resident protein (Fig. 9B).

DISCUSSION

The product of the H7R ORF was shown to be a 17-kDa protein expressed following VACV DNA replication. Unlike many viral late proteins, H7 was not present in appreciable amounts in purified virus particles, nor did it localize to specific cellular organelles. Although the conservation of H7 homologs in all sequenced chordopoxviruses suggested its importance in the virus life cycle, there were no discernible functional motifs or nonpoxvirus homologs. To gain insight into the role of H7, we made a recombinant virus in which synthesis of the protein was stringently dependent on IPTG. The mutant exhibited a conditional lethal phenotype; i.e., formation of infectious virus was dependent on inducer. In the absence of inducer, viral protein synthesis appeared normal except for a defect in processing of certain membrane and core proteins. Processing of VACV proteins is dependent on morphogenesis, and the failure of the A17 membrane protein, as well as core proteins, to be cleaved by the I7 protease suggested a block at a very early stage (2). Large spherical inclusions containing viral core proteins were detected within cytoplasmic factories by confocal microscopy. The inclusions were very dense since antibodies could bind only to their surfaces, giving the appearance of rings in Z-sections. Corresponding dense inclusions were seen by transmission electron microscopy of cell sections and were shown by immunogold staining to contain core proteins. Crescent membranes and IVs were not seen although some dense inclusions had membrane segments partially coated with spicules, presumably composed of D13 trimers, at their surfaces. However, most of the D13 scaffold protein was present in separate intermediate density inclusions that were associated with ER membranes, as shown by immunogold labeling. We are unsure whether the primary defect is in membrane formation and the membrane segments are due to trace amounts of H7 synthesized in the absence of IPTG (though this was not detected by Western blotting) or whether the membrane segments form inefficiently despite the absence of H7.

Of the various VACV mutants, the H7 mutant described here is most similar to the inducible A11 mutant previously studied in our laboratory (28). A11 with a mass of 40 kDa is larger than H7 but is also expressed late in infection and is not incorporated into MVs. When A11 was repressed, processing of the A17 membrane protein and core proteins was inhibited, and neither crescents nor IVs formed. Electron-dense inclusions containing core proteins and intermediate-density inclusions containing D13 and ER membranes as well as the A17 IV membrane protein were present. Also, the L1 membrane protein was present in very small amounts when either H7 or A11 was repressed, suggesting that viral membranes are needed for their stability. However, H7 and A11 have no sequence homology, and we have been unable to demonstrate an interaction between them by immunoprecipitation (P. S. Satheshkumar, unpublished observations). Nevertheless, it seems likely that H7 and A11 function at the same time or in closely related steps in morphogenesis. The roles of H7 and A11 in viral membrane formation are particularly intriguing as neither pro-

FIG. 7. Confocal microscopy of cells infected with mutant viruses. HeLa cells were grown on coverslips and infected with vH7-HAi (A and B) or with vT7LacOI, vA9Li, or vAllRi (C) in the absence (−) or presence (+) of 100 μM IPTG, as indicated. Cells were fixed after 18 h, permeabilized, and stained with antibodies to GFP, HA (for H7), L1, or A4 or with DAPI. In panel A, GFP was also localized by fluorescence. F, virus factory; Nu, nucleus.

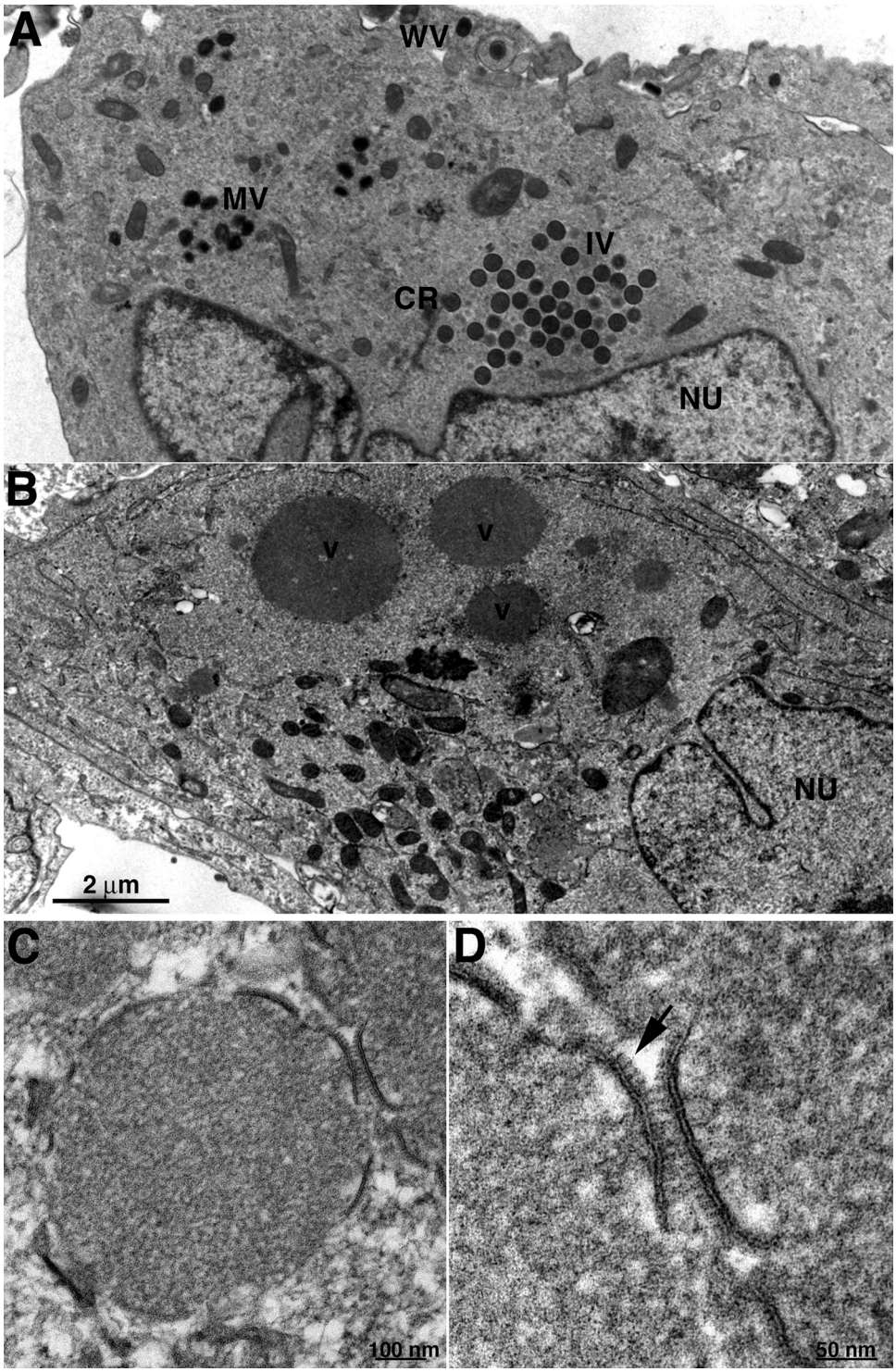

FIG. 8. Transmission electron microscopy of cells infected with vH7-HAi. BS-C-1 cells were infected with 3 PFU per cell of vH7-HAi in the presence or absence of IPTG for 20 h and then prepared for transmission electron microscopy. (A) Cells with IPTG. (B) Cells without IPTG. (C) Electron-dense inclusion with associated membrane segments that formed in the absence of IPTG. (D) Higher magnification of membrane segments from panel C; the arrow points to spicules. CR, crescent; WV, wrapped virion; V, dense inclusion of viroplasm; Nu, nucleus. Magnifications are indicated by scale bars.

tein is associated with viral membranes, packaged in virus particles, or has obvious catalytic motifs.

Several other VACV mutants also show defects in viral membrane formation. Temperature-sensitive G5 and H5 mutants fail to form crescents and IVs at nonpermissive conditions (7, 12). However, these proteins are also expressed early in infection and have additional roles, making it possible that the effect on morphogenesis is indirect (4, 11, 22) (T. Senkev-

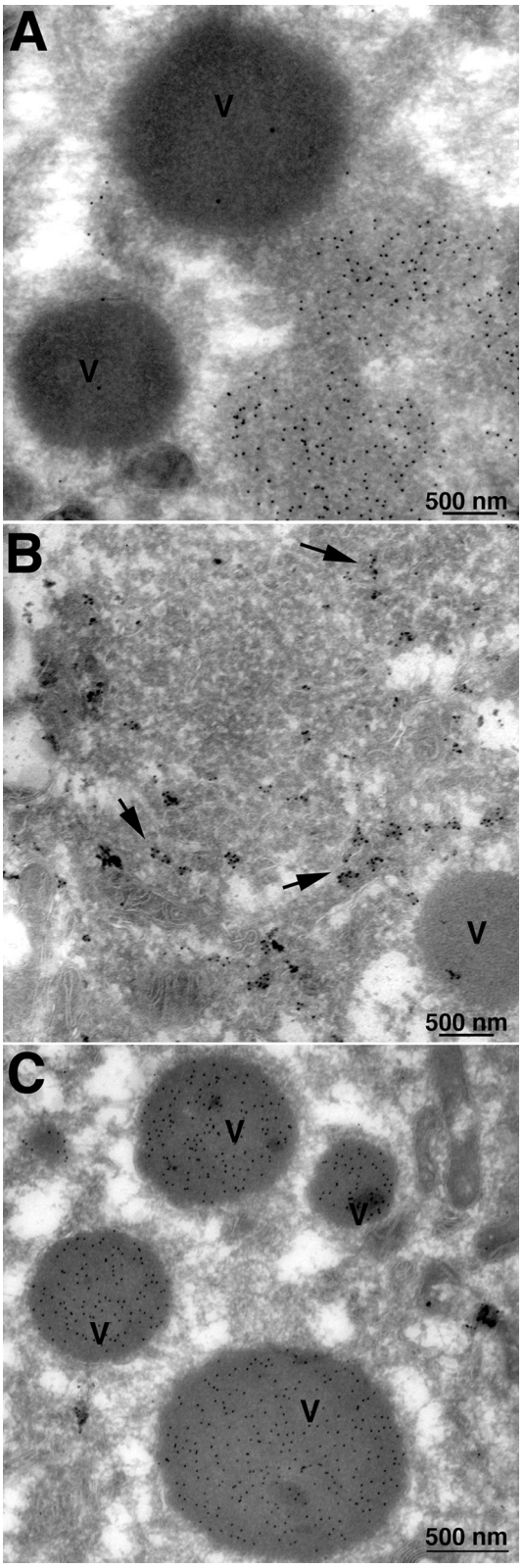

FIG. 9. Immunogold electron microscopy of inclusions. Cells were infected with vH7-HAi in the absence of IPTG as described in the legend to Fig. 8. Thawed cryosections were incubated with antibodies to the D13 scaffold protein (A), the ER-resident protein disulfide isomerase (B), and the A3 core protein (C), followed by protein A conjugated to colloidal gold. Arrows point to gold spheres in panel B.

ich, unpublished observations). Temperature-sensitive F10 mutants also have a defect in viral membrane formation (37, 38). Repression of A17 and A14 perturbs viral membrane formation, but the vesicles and tubules that form are not seen with the other mutants (30, 31, 39, 41). It remains to be determined whether all of the viral proteins that contribute directly to viral membrane formation are now known.

ACKNOWLEDGMENTS

We thank Elizabeth Fischer, Rocky Mountain Laboratories, National Institute of Allergy and Infectious Diseases (NIAID), for initial electron microscopy analysis; Cindy Sood for vI5-HA virus; Catherine Cotter for tissue culture cells; and the NIAID biological imaging facility.

The research was supported by the Division of Intramural Research of the NIAID, National Institutes of Health.

REFERENCES

1. **Alexander, W. A., B. Moss, and T. R. Fuerst.** 1992. Regulated expression of foreign genes in vaccinia virus under the control of bacteriophage T7 RNA polymerase and the *Escherichia coli lac* repressor. J. Virol. **66:**2934–2942.
2. **Ansarah-Sobrinho, C., and B. Moss.** 2004. Role of the I7 protein in proteolytic processing of vaccinia virus membrane and core components. J. Virol. **78:**6335–6343.
3. **Betakova, T., E. J. Wolffe, and B. Moss.** 1999. Regulation of vaccinia virus morphogenesis: phosphorylation of the A14L and A17L membrane proteins and C-terminal truncation of the A17L protein are dependent on the F10L protein kinase. J. Virol. **73:**3534–3543.
4. **Black, E. P., N. Moussatche, and R. C. Condit.** 1998. Characterization of the interactions among vaccinia virus transcription factors G2R, A18R, and H5R. Virology **245:**313–322.
5. **Chichon, F. J., M. J. Rodriguez, C. Risco, A. Fraile-Ramos, J. J. Fernandez, M. Esteban, and J. L. Carrascosa.** 2009. Membrane remodeling during vaccinia virus morphogenesis. Biol. Cell **101:**401–414.
6. **Condit, R. C., N. Moussatche, and P. Traktman.** 2006. In a nutshell: structure and assembly of the vaccinia virion. Adv. Virus Res. **66:**31–124.
7. **Da Fonseca, F. G., A. S. Weisberg, M. F. Caeiro, and B. Moss.** 2004. Vaccinia virus mutants with alanine substitutions in the conserved G5R gene fail to initiate morphogenesis at the nonpermissive temperature. J. Virol. **78:**10238–10248.
8. **Dales, S.** 1963. The uptake and development of vaccinia virus in strain L cells followed with labeled viral deoxyribonucleic acid. J. Cell Biol. **18:**51–72.
9. **Dales, S., and E. H. Mosbach.** 1968. Vaccinia as a model for membrane biogenesis. Virology **35:**564–583.
10. **Dales, S., and L. Siminovitch.** 1961. The development of vaccinia virus in Earle's L strain cells as examined by electron microscopy. J. Biophys. Biochem. Cytol. **10:**475–503.
11. **D'Costa, S. M., T. W. Bainbridge, and R. C. Condit.** 2008. Purification and properties of the vaccinia virus mRNA processing factor. J. Biol. Chem. **283:**5267–5275.
12. **DeMasi, J., and P. Traktman.** 2000. Clustered charge-to-alanine mutagenesis of the vaccinia virus H5 gene: isolation of a dominant, temperature-sensitive mutant with a profound defect in morphogenesis. J. Virol. **74:**2393–2405.
13. **Derrien, M., A. Punjabi, R. Khanna, O. Grubisha, and P. Traktman.** 1999. Tyrosine phosphorylation of A17 during vaccinia virus infection: involvement of the H1 phosphatase and the F10 kinase. J. Virol. **73:**7287–7296.
14. **Earl, P. L., N. Cooper, L. S. Wyatt, B. Moss, and M. W. Carroll.** 1998. Preparation of cell cultures and vaccinia virus stocks, p. 16.16.1–16.16.3. *In* F. M. Ausubel, R. Brent, R. E. Kingston, D. D. Moore, J. G. Seidman, J. A. Smith, and K. Struhl (ed.), Current protocols in molecular biology, vol. 2. John Wiley and Sons, New York, NY.
15. **Earl, P. L., and B. Moss.** 1998. Characterization of recombinant vaccinia viruses and their products, p. 16.18.1–16.18.11. *In* F. M. Ausubel, R. Brent, R. E. Kingston, D. D. Moore, J. G. Seidman, J. A. Smith, and K. Struhl (ed.), Current protocols in molecular biology, vol. 2. Wiley Interscience, New York, NY.
16. **Earl, P. L., B. Moss, L. S. Wyatt, and M. W. Carroll.** 1998. Generation of recombinant vaccinia viruses, p. 16.17.1–16.17.19. *In* F. M. Ausubel, R. Brent, R. E. Kingston, D. D. Moore, J. G. Seidman, J. A. Smith, and K. Struhl (ed.), Current protocols in molecular biology, vol. 2. Wiley Interscience, New York, NY.
17. **Grimley, P. M., E. N. Rosenblum, S. J. Mims, and B. Moss.** 1970. Interruption by rifampin of an early stage in vaccinia virus morphogenesis: accumulation of membranes which are precursors of virus envelopes. J. Virol. **6:**519–533.
18. **Heuser, J.** 2005. Deep-etch EM reveals that the early poxvirus envelope is a

single membrane bilayer stabilized by a geodetic "honeycomb" surface coat. J. Cell Biol. **169:**269–283.
19. **Hollinshead, M., A. Vanderplasschen, G. L. Smith, and D. J. Vaux.** 1999. Vaccinia virus intracellular mature virions contain only one lipid membrane. J. Virol. **73:**1503–1517.
20. **Husain, M., and B. Moss.** 2003. Evidence against an essential role of COPII-mediated cargo transport to the endoplasmic reticulum-Golgi intermediate compartment in the formation of the primary membrane of vaccinia virus. J. Virol. **77:**11754–11766.
21. **Husain, M., A. S. Weisberg, and B. Moss.** 2006. Existence of an operative pathway from the endoplasmic reticulum to the immature poxvirus membrane. Proc. Natl. Acad. Sci. USA **103:**19506–19511.
22. **Kovacs, G. R., and B. Moss.** 1996. The vaccinia virus H5R gene encodes late gene transcription factor 4: purification, cloning and overexpression. J. Virol. **70:**6796–6802.
23. **Mercer, J., and P. Traktman.** 2003. Investigation of structural and functional motifs within the vaccinia virus A14 phosphoprotein, an essential component of the virion membrane. J. Virol. **77:**8857–8871.
24. **Mohandas, A. R., and S. Dales.** 1995. Involvement of spicules in the formation of vaccinia virus envelopes elucidated by a conditional lethal mutant. Virology **214:**494–502.
25. **Moss, B.** 2007. *Poxviridae*: the viruses and their replication, p. 2905–2946. *In* D. M. Knipe, P. M. Howley, D. E. Griffin, R. A. Lamb, M. A. Martin, B. Roizman, and S. E. Straus (ed.), Fields virology, 5th ed., vol. 2. Lippincott Williams & Wilkins, Philadelphia, PA.
26. **Moss, B., E. N. Rosenblum, E. Katz, and P. M. Grimley.** 1969. Rifampicin: a specific inhibitor of vaccinia virus assembly. Nature **224:**1280–1284.
27. **Nelson, G. E., J. R. Sisler, D. Chandran, and B. Moss.** 2008. Vaccinia virus entry/fusion complex subunit A28 is a target of neutralizing and protective antibodies. Virology **380:**394–401.
28. **Resch, W., A. S. Weisberg, and B. Moss.** 2005. Vaccinia virus nonstructural protein encoded by the A11R gene is required for formation of the virion membrane. J. Virol. **79:**6598–6609.
29. **Risco, C., J. R. Rodriguez, C. Lopez-Iglesias, J. L. Carrascosa, M. Esteban, and D. Rodriguez.** 2002. Endoplasmic reticulum-Golgi intermediate compartment membranes and vimentin filaments participate in vaccinia virus assembly. J. Virol. **76:**1839–1855.
30. **Rodríguez, D., M. Esteban, and J. R. Rodríguez.** 1995. Vaccinia virus A17L gene product is essential for an early step in virion morphogenesis. J. Virol. **69:**4640–4648.
31. **Rodriguez, J. R., C. Risco, J. L. Carrascosa, M. Esteban, and D. Rodriguez.** 1998. Vaccinia virus 15-kilodalton (A14L) protein is essential for assembly and attachment of viral crescents to virosomes. J. Virol. **72:**1287–1296.
32. **Senkevich, T. G., L. S. Wyatt, A. S. Weisberg, E. V. Koonin, and B. Moss.** 2008. A conserved poxvirus NlpC/P60 superfamily protein contributes to vaccinia virus virulence in mice but not to replication in cell culture. Virology **374:**506–514.
33. **Sodeik, B., R. W. Doms, M. Ericsson, G. Hiller, C. E. Machamer, W. van't Hof, G. van Meer, B. Moss, and G. Griffiths.** 1993. Assembly of vaccinia virus: role of the intermediate compartment between the endoplasmic reticulum and the Golgi stacks. J. Cell Biol. **121:**521–541.
34. **Sodeik, B., and J. Krijnse-Locker.** 2002. Assembly of vaccinia virus revisited: de novo membrane synthesis or acquisition from the host? Trends Microbiol. **10:**15–24.
35. **Sood, C. L., J. M. Ward, and B. Moss.** 2008. Vaccinia virus encodes a small hydrophobic virion membrane protein (I5) that enhances replication and virulence in mice. J. Virol. **82:**10071–10078.
36. **Szajner, P., A. S. Weisberg, J. Lebowitz, J. Heuser, and B. Moss.** 2005. External scaffold of spherical immature poxvirus particles is made of protein trimers, forming a honeycomb lattice. J. Cell Biol. **170:**971–981.
37. **Szajner, P., A. S. Weisberg, and B. Moss.** 2004. Evidence for an essential catalytic role of the F10 protein kinase in vaccinia virus morphogenesis. J. Virol. **78:**257–265.
38. **Traktman, P., A. Caligiuri, S. A. Jesty, and U. Sankar.** 1995. Temperature-sensitive mutants with lesions in the vaccinia virus F10 kinase undergo arrest at the earliest stage of morphogenesis. J. Virol. **69:**6581–6587.
39. **Traktman, P., K. Liu, J. DeMasi, R. Rollins, S. Jesty, and B. Unger.** 2000. Elucidating the essential role of the A14 phosphoprotein in vaccinia virus morphogenesis: construction and characterization of a tetracycline-inducible recombinant. J. Virol. **74:**3682–3695.
40. **Upton, C., S. Slack, A. L. Hunter, A. Ehlers, and R. L. Roper.** 2003. Poxvirus orthologous clusters: toward defining the minimum essential poxvirus genome. J. Virol. **77:**7590–7600.
41. **Wolffe, E. J., D. M. Moore, P. J. Peters, and B. Moss.** 1996. Vaccinia virus A17L open reading frame encodes an essential component of nascent viral membranes that is required to initiate morphogenesis. J. Virol. **70:**2797–2808.
42. **Yeh, W. W., B. Moss, and E. J. Wolffe.** 2000. The vaccinia virus A9L gene encodes a membrane protein required for an early step in virion morphogenesis. J. Virol. **74:**9701–9711.
43. **Zhang, L. L., S. Y. Lee, G. V. Beznoussenko, P. J. Peters, J. S. Yang, H. Y. Gilbert, A. L. Brass, S. J. Elledge, S. N. Isaacs, B. Moss, A. Mironov, and V. W. Hsu.** 2009. A role for the host coatomer and KDEL receptor in early vaccinia biogenesis. Proc. Natl. Acad. Sci. USA **106:**163–168.
44. **Zhang, Y., and B. Moss.** 1992. Immature viral envelope formation is interrupted at the same stage by *lac* operator-mediated repression of the vaccinia virus D13L gene and by the drug rifampicin. Virology **187:**643–653.